IJRAR.ORG E-ISSN: 2348-1269, P-ISSN: 2349-5138

INTERNATIONAL JOURNAL OF RESEARCH AND ANALYTICAL REVIEWS (IJRAR) | IJRAR.ORG

An International Open Access, Peer-reviewed, Refereed Journal

Integrated molecular and elemental profiling of *AchyranthesAspera Linn.* Through FTIR, UV–Vis, XRF, And LC–MS: Insights Into Its Phytochemical Architecture And Therapeutic Potential

Nirav Sadhu[1]*, M.V.Parsania[2], Rupak Dey[3], Vishvaraj vala[4] and Jyotindra Bhatt[5]

[1]Research Scholar, [2]Associate Professor, [3]Project Scientist, [4]Research Scholar, [5]Associate Professor

[1,3]Gujarat Institute of Desert Ecology, Bhuj, Gujarat, India

[2]Department of chemistry, M.G. Science Institute, Ahmedabad, Gujarat, India

[4,5]Department of Chemistry, K.S.K.V. Kachchh University Bhuj, Gujarat, india

Abstract

Achyranthesaspera Linn. (Amaranthaceae), a key Ayurvedic species, is renowned for anti-inflammatory, antidiabetic, and hepatoprotective activities, yet lacks a unified instrumental characterization. This study integrates Fourier-Transform Infrared (FTIR), Ultraviolet–Visible (UV–Vis), X-Ray Fluorescence (XRF), and Liquid Chromatography–Mass Spectrometry (LC–MS) to delineate the phytochemical and elemental architecture of the plant.

FTIR spectra (4000–400 cm^{-1}) exhibited major peaks at 3346, 3244, 2931, 2866, 1635, 1033, and 875 cm^{-1}, signifying hydroxyl, carbonyl, and aromatic functionalities typical of flavonoids, phenolics, and glycosides. UV–Vis absorbance maxima at 274 nm with shoulders near 230–260 nm and 340 nm confirmed conjugated π–π* and n–π* transitions. XRF profiling demonstrated a mineral-rich matrix dominated by K_2O (44.9 %), CaO (23.6 %), and MgO (5.93 %), alongside trace Fe_2O_3, ZnO, MnO, and CuO. LC–MS analysis (ES^+/ES^-, m/z 59–1195) resolved multiple alkaloid classes ranging from simple amines to triterpenoid–glycosidic conjugates.

This multi-modal fingerprint validates traditional claims and offers reproducible analytical markers for quality control, chemotaxonomy, and future bioactivity-guided isolation

Keywords: *AchyranthesasperaLinn.*, FTIR, UV–Vis, XRF, LC–MS, Phytochemical Profiling, Alkaloids, Elemental Analysis, Pharmacognosy.

1. Introduction

Medicinal plants represent a vital source of structurally diverse bioactive compounds and continue to play a pivotal role in both traditional medicine and modern drug discovery. Amongst these, *Achyranthesaspera* Linn. (familyAmaranthaceae), commonly known as Prickly Chaff Flower, is of particular importance in Indian ethnomedicine and is well documented in the Ayurvedic pharmacopoeia. This perennial herb is widely distributed throughout tropical and subtropical regions of Asia, Africa, and the Americas. Traditionally, *A. aspera* has been used in the treatment of various ailments, including inflammatory disorders, asthma, diabetes, hypertension, jaundice, cough, and skin diseases. Importantly, all parts of the plant—roots, stems, leaves, and seeds—have been reported to exhibit medicinal properties, which are primarily attributed to the presence of a diverse array of secondary metabolites.(Dutt et al., 2010; Gokhale et al., 2002; Isha Talhar et al., 2025; Nargatti et al., 2021; Singh et al., 2021)

Phytochemical studies on *Achyranthesaspera* have demonstrated the presence of a wide range of bioactive constituents, including alkaloids, flavonoids, saponins, glycosides, terpenoids, and phenolic compounds.(Nargatti et al., 2021) These phytochemicals are collectively associated with the plant's diverse pharmacological activities, such as anti-inflammatory, antimicrobial, hepatoprotective, antidiabetic, and antioxidant effects.(Gokhale et al., 2002; Vijaya Kumar et al., 2009) Despite these findings, comprehensive and comparative analytical profiling of *A. aspera* using advanced chromatographic and spectroscopic techniques remains limited. A detailed understanding of its molecular and elemental composition is therefore crucial for substantiating traditional therapeutic claims, ensuring safety and quality, and supporting the standardization of this plant for phytopharmaceutical and drug development applications(Harborne&Harborne, 1998; Sofowora et al., 2013).

In this context, the present study undertakes a comprehensive, multidimensional analytical profiling of *Achyranthesaspera* Linn. using Fourier Transform Infrared (FTIR) spectroscopy, Ultraviolet–Visible (UV–Vis) spectroscopy, X-ray fluorescence (XRF) spectroscopy, and liquid chromatography–mass spectrometry (LC–MS).(Harborne & Harborne, 1998; Qureshi & Solanki, 2022; Silverstein et al., 2015; Towett et al., 2016) These complementary techniques collectively provide detailed insights into the plant's chemical and elemental composition. FTIR spectroscopy was employed to identify characteristic functional groups and structural motifs, confirming the presence of hydroxyl, carbonyl, and aromatic moieties associated with phenolics, flavonoids, and glycosides. UV–Vis spectroscopy revealed diagnostic absorption bands corresponding to π–π* and n–π* electronic transitions, indicative of conjugated aromatic and polyphenolic systems linked to antioxidant activity. XRF spectroscopies enabled the determination of elemental and mineral composition, allowing the quantification of major and trace oxides, including K_2O, CaO, MgO, Fe_2O_3, ZnO, and related constituents, thereby highlighting the plant's nutritional and therapeutic relevance. LC–MS analysis provided detailed molecular profiling of complex alkaloid and triterpenoid constituents by elucidating molecular ion distributions and fragmentation patterns over a wide *m/z* range (59–1195), resulting in a robust chemical fingerprint.(Dettmer et al., 2007; Niessen, 2006; Wolfender et al., 2015)

This integrative analytical strategy affords a comprehensive chemical and elemental characterization of *A. aspera*, effectively linking its traditional medicinal applications with scientifically validated molecular evidence. Such systematic characterization enhances the chemotaxonomic understanding of the species, supports its pharmacognostic standardization, and reinforces its potential as a valuable source of novel natural therapeutic agents.

Previous investigations on *Achyranthesaspera* have established the presence of a variety of bioactive constituents, including alkaloids, flavonoids, tannins, saponins, and steroids, thereby substantiating its ethnomedicinal significance. Several chromatographic studies, primarily employing thin-layer chromatography (TLC) and limited high-performance liquid chromatography (HPLC), have reported partial characterization of selected metabolites; however, these analyses were often confined to specific solvent extracts or isolated compounds.(Dutt et al., 2010; Nargatti et al., 2021; Skoog et al., 2018; Snyder et al., 2009; Stahl, 1969; Towett et al., 2016) Similarly, earlier spectroscopic investigations, such as infrared (IR) and ultraviolet (UV) analyses, provided preliminary insights into functional group composition but lacked detailed spectral interpretation, comparative evaluation, and comprehensive profiling across different plant parts. In contrast, studies addressing the elemental composition of *A. aspera* remain relatively scarce, and advanced non-destructive techniques such as X-ray fluorescence (XRF) spectroscopy have been underutilized, despite their relevance for assessing essential and trace elements that may influence therapeutic efficacy and safety.(Lindon et al., 2017; Sapkota et al., 2019)

Collectively, the existing literature highlights notable research gaps. Although the pharmacological potential of *A. aspera* is well recognized, comprehensive chemical fingerprinting that integrates advanced spectroscopic and chromatographic approaches, including FTIR, HPLC, and XRF analyses, remains largely unexplored. There is a clear need for an in-depth and systematic investigation that (i) correlates spectroscopic and chromatographic data to identify reliable marker compounds, (ii) evaluates variations in phytochemical composition across different plant parts or extraction systems, and (iii) profiles elemental constituents to elucidate their contribution to biological activity. Such an instrumentally rigorous and integrative study would significantly advance the chemotaxonomic understanding, quality control, and standardization of *A. aspera*, thereby supporting its future pharmacognostic and phytopharmaceutical applications.

The present study is designed to conduct a comprehensive phytochemical screening of *Achyranthesaspera* Linn. with the objective of identifying the major classes of bioactive constituents. Fourier Transform Infrared (FTIR) spectroscopy is employed to record and interpret spectral data for the characterization of functional groups and the establishment of molecular fingerprints of plant extracts. In addition, high-performance liquid chromatography (HPLC) is utilized for the qualitative and quantitative profiling of phytoconstituents and for the identification of potential marker compounds. The study further aims to determine the elemental composition of *A. aspera* using X-ray fluorescence (XRF) analysis, with particular emphasis on assessing the significance of macro- and micro-elements in relation to therapeutic potential. Finally, data obtained from FTIR, HPLC, and XRF analyses are integrated to generate a comprehensive chemical and elemental profile that can support future pharmacological investigations and formulation-oriented research.

2. Materials and methods

2.1. Field Survey, Collection, and Taxonomical Identification

Fresh plant materials of *Achyranthesaspera* Linn.was collected from the Bhuj region of Gujarat, India. The botanical identity of the species was authenticated by a qualified taxonomist from the Department of Botany, K.S.K.V. Kachchh University, and a voucher specimen (Accession No. AA-NIR-2018) was deposited in the departmental herbarium for future reference. Following collection, the plant material was thoroughly washed to remove extraneous matter, shade-dried under ambient conditions, and subsequently ground into a uniform fine powder to facilitate extraction and subsequent analytical investigations.

2.2. Preparation of Solvent Extraction

Powdered plant material (10 g) was extracted using methanol, ethanol, or hexane, selected according to the specific analytical objectives of the study. The extraction was carried out either by Soxhlet extraction or by maceration, as appropriate. Following extraction, the solutions were filtered through Whatman No. 1 filter paper and concentrated under reduced pressure using a rotary evaporator. The resulting dried extracts were stored at 4 °C until further spectroscopic and chromatographic analyses.(Harborne& Harborne, 1998; Stalikas, 2007)

2.3. FTIR Spectral Analysis

Fourier Transform Infrared (FTIR) spectra were acquired using a Shimadzu FTIR-8400S spectrophotometer equipped with an attenuated total reflectance (ATR, KRS-5) accessory, over the spectral range of 4000–400 cm^{-1}. Samples were analyzed either as potassium bromide (KBr) pellets or directly as thin films, depending on the physical nature of the extract. Prominent absorption bands were identified and assigned to their corresponding functional groups by comparison with standard spectral databases and published literature.

2.4. UV-Vis Spectral Analysis

Ultraviolet–visible (UV–Vis) spectra were recorded using a Shimadzu UV-3600 double-beam spectrophotometer. The absorbance spectrum of the hexane extract was measured over the wavelength range of 190–800 nm using a slit width of 8 nm. Characteristic maximum absorption wavelengths (λ_{max}) were documented to assess the presence of conjugated chromophoric systems commonly associated with flavonoids, phenolic compounds, and terpenoids.

2.5. X-Ray Fluorescence (XRF) Spectral Analysis

The elemental and mineral composition of *Achyranthesaspera* was determined using an energy-dispersive X-ray fluorescence (EDXRF) spectrometer (PANalyticalAxiosmAX, Netherlands). Finely powdered plant ash was pelletized and analyzed for the presence of major and trace elemental oxides. Quantitative results were expressed as mass percentages of MgO, Al_2O_3, SiO_2, P_2O_5, SO_3, Cl, K_2O, CaO, along with other trace elements. Instrument calibration was carried out using certified reference materials to ensure analytical accuracy and reliability.

2.6. Liquid Chromatography-Mass Spectrometry (LC-MS) spectral Analysis

The alkaloid-rich fraction was analyzed using a Waters XEVO TQD triple-quadrupole liquid chromatography–mass spectrometry (LC–MS) system equipped with an electrospray ionization (ESI) source operated in both positive and negative ionization modes. Chromatographic separation was performed on a reversed-phase C18 column (150 × 4.6 mm, 5 µm) using a gradient elution program with acetonitrile and water containing 0.1% formic acid as the mobile phase. The total ion chromatogram (TIC) was acquired over a retention time window of 2–12 min, and molecular ion signals in the *m/z* range of 59–1195 were evaluated for compound identification and structural interpretation.

2.7. Data Analysis

Spectral and chromatographic data were processed and analyzed using OriginPro and MassLynx software packages. All experiments were conducted in triplicate, and the results are presented as mean ± standard deviation (SD). Identification and interpretation of functional groups, elemental concentrations, and molecular fragmentation patterns were carried out by comparison with reported literature data and established spectral databases, including the NIST and Wiley libraries.

3. Results

3.1 .FTIR Spectral Analysis

The FTIR spectrum of the *Achyranthesaspera* Linn.extract, recorded over the range of 4000–400 cm^{-1}, exhibited a complex pattern of absorption bands characteristic of plant-derived secondary metabolites. The transmittance profile showed prominent peaks at approximately 3346, 3244, 3151, 2931, 2866, 2449, 2299, 1635, 1033, and 875 cm^{-1}, indicating the presence of a chemically diverse mixture of organic constituents within the extract.

A broad absorption envelope observed in the region of 3346–3244 cm^{-1} is attributed to O–H stretching vibrations, suggesting the occurrence of hydroxyl-containing functional groups typical of alcohols, phenols, and carboxylic acids. Such groups are commonly associated with flavonoids, tannins, and saponins and are indicative of strong hydrogen-bonding interactions. The medium-intensity bands appearing between 2931 and 2866 cm^{-1} correspond to aliphatic C–H stretching vibrations of $–CH_2$ and $–CH_3$ groups, implying the presence of long-chain hydrocarbons, terpenoids, and lipid-like constituents.

A sharp and intense absorption band near 1635 cm^{-1} is characteristic of C=O stretching vibrations of conjugated carbonyl groups, as found in flavonoids, ketones, and carboxylic acids, as well as C=C stretching vibrations of aromatic rings. This feature reflects the polyphenolic nature of the extract. The absorption band at approximately 1033 cm^{-1} is assigned to C–O–C stretching vibrations, indicative of glycosidic linkages or polysaccharide structures, while the weak band around 875 cm^{-1} may be attributed to C–H bending vibrations of aromatic systems or substituted alkenes.

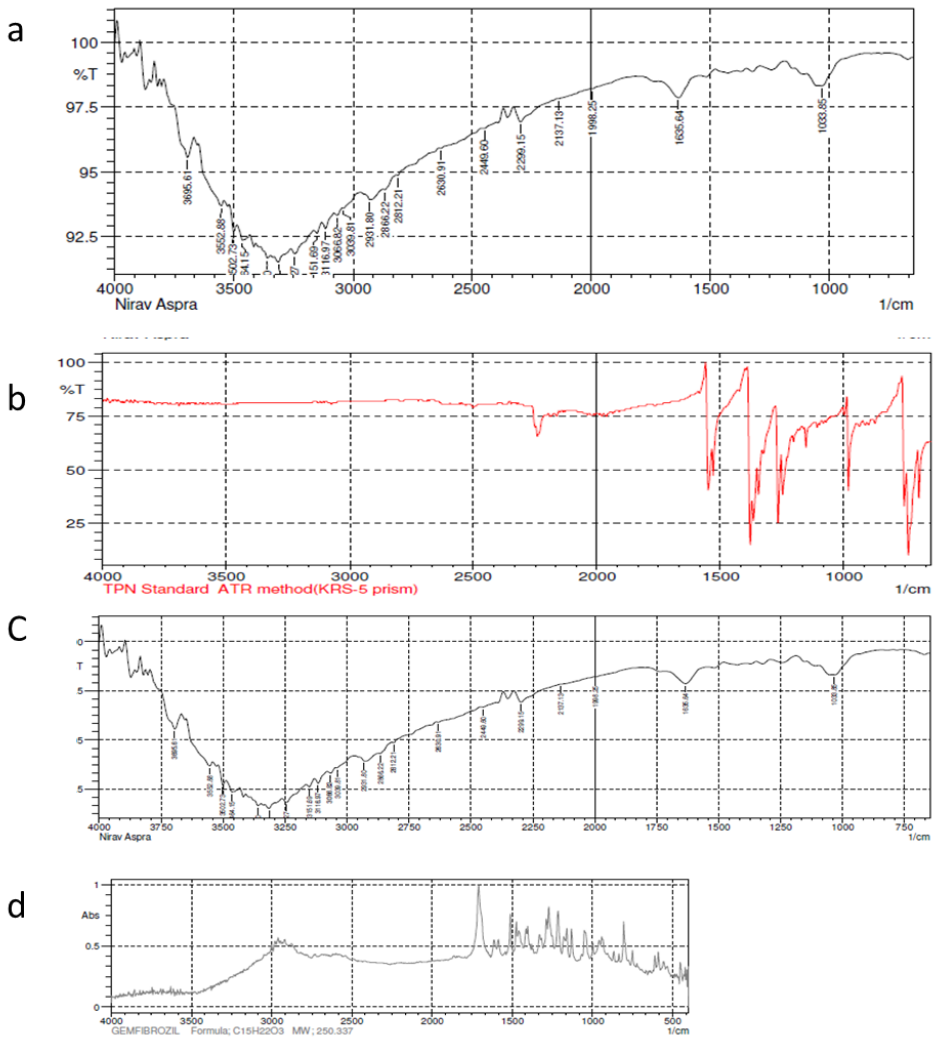

Figure 1: Fourier-Transform Infrared Spectroscopy (FTIR) spectrum

Collectively, these FTIR spectral features confirm the presence of major phytochemical classes, including flavonoids, saponins, terpenoids, phenolic compounds, and glycosides, in *A. aspera*. The observed functional group assignments are in close agreement with previously reported FTIR analyses of *A. aspera* leaves and whole plant extracts, thereby corroborating the consistency and reliability of the present findings (Table 1).

Table 1: FTIR spectral peak values and functional groups

Peak (cm^{-1})	**Intensity (%T)**	**Probable functional group**	**Assignment / Inference**
3346	Strong, broad	O–H stretching	Alcohols, phenols (hydrogen bonding)
3244	Broad	N–H stretching	Amines, amides, proteins
2931	Medium	C–H asymmetric stretching	Aliphatic CH_2 groups, terpenoids, lipids
2866	Medium	C–H symmetric stretching	Alkanes, fatty acids
2449	Weak	C≡ N / O–H overtone	Nitriles / hydrogen bonding
2299	Weak	C≡ C stretching	Alkynes or unsaturated compounds
1635	Strong	C=O stretching / C=C aromatic	Carbonyls, flavonoids, phenolics
1033	Medium	C–O–C stretching	Alcohols, ethers, glycosides
875	Weak	C–H bending (aromatic)	Alkenes, substituted benzene rings

3.2. Library Match Analysis

The ATR–FTIR spectral data were further compared with the instrument's reference library, yielding notable similarity scores with standard spectra of compounds such as gemfibrozil, dioctyl phthalate, isopropyl ether, and olive oil. Although these matches do not indicate the direct presence of the referenced compounds, they suggest the occurrence of structurally related functional moieties, particularly aliphatic esters, fatty acids, and lipid-like constituents. Such chemical features are characteristic of plant waxes and lipid-associated secondary metabolites. The detection of these compound classes is consistent with, and provides a molecular basis for, the antimicrobial and antioxidant activities previously reported for Achyranthesaspera extracts.

3.3. X-Ray Fluorescence (XRF) Spectral Analysis

The elemental profile of *Achyranthesaspera* Linn.powder was examined using X-ray fluorescence (XRF) spectroscopy to obtain both qualitative and quantitative information on its major, minor, and trace inorganic constituents. The resulting XRF spectra displayed well-resolved characteristic emission peaks corresponding to multiple elements, confirming the mineral-rich nature of the plant material (Figure 2). Quantitative elemental concentrations, expressed as mass percentages of their respective oxides, are presented in Table 2.

Potassium (K_2O, 44.90%) and calcium (CaO, 23.60%) were identified as the predominant constituents, together constituting the major portion of the mineral composition of *A. aspera*. Potassium is known to play a central role in enzymatic activation, osmotic balance, and water regulation in plants, whereas calcium is essential for maintaining cell wall architecture, membrane integrity, and intracellular signaling pathways. The high abundance of these macronutrients underscores the nutritional significance and therapeutic potential of the plant.

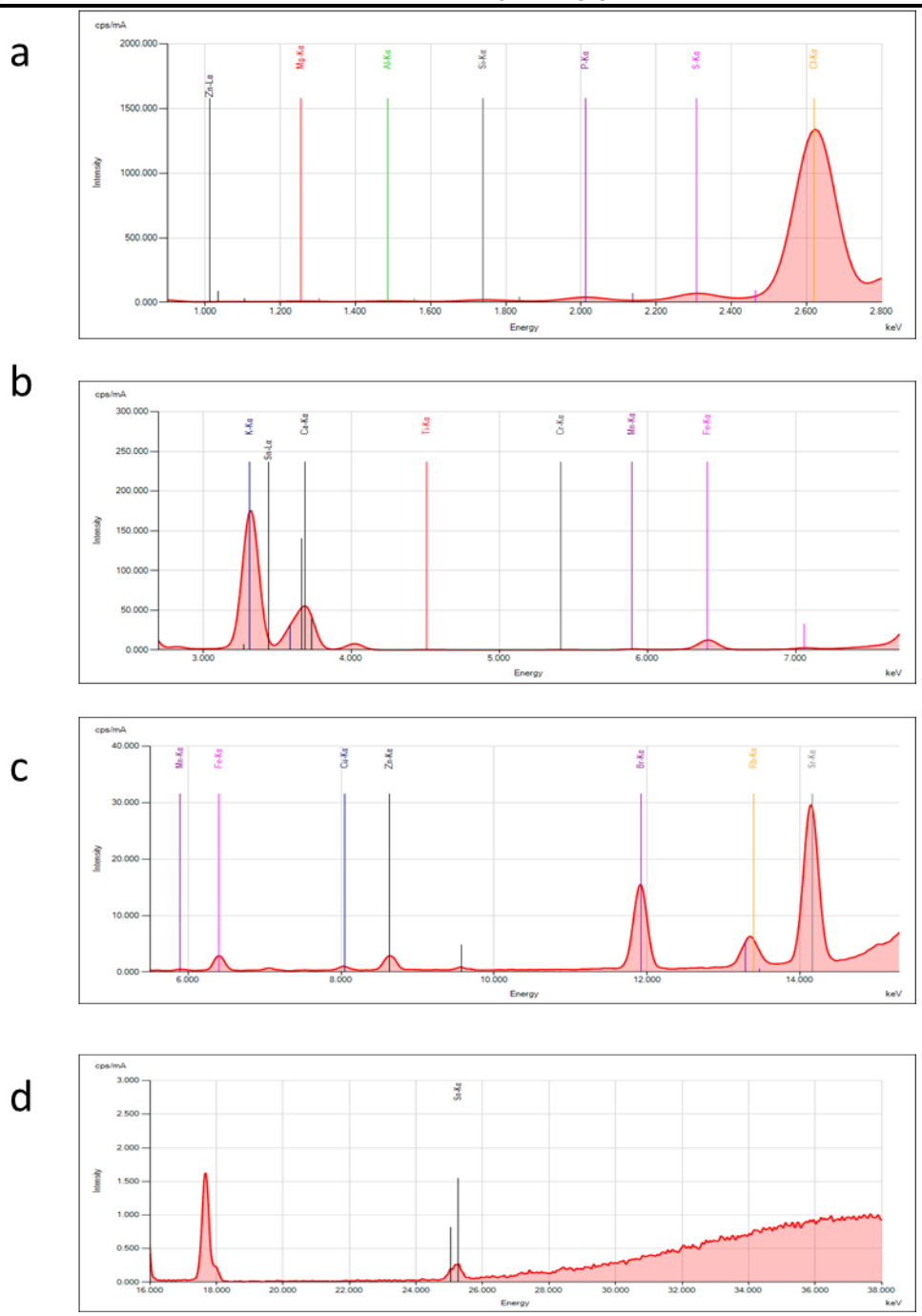

Figure 2: X-ray fluorescence (XRF) spectra of *Achyranthesaspera* Linn. powder showing the characteristic emission peaks corresponding to major, minor, and trace elements across different energy ranges, confirming the mineral-rich elemental composition of the plant material.

In addition to these major elements, moderate amounts of magnesium oxide (MgO, 5.93%), silicon dioxide (SiO_2, 2.35%), phosphorus pentoxide (P_2O_5, 2.00%), sulphur trioxide (SO_3, 2.70%), and chlorine (Cl, 15.00%) were detected. Magnesium functions as an important cofactor for numerous enzymes and is a key component of chlorophyll, while phosphorus is indispensable for energy transfer processes and nucleic acid biosynthesis. Sulphur contributes to the synthesis of sulphur-containing amino acids and coenzymes, and silicon is associated with improved structural rigidity and enhanced resistance to biotic stress. The relatively elevated chlorine content may be linked to its role in regulating ionic equilibrium and osmotic potential within plant tissues.

Several minor and trace elements were also identified, including iron (Fe_2O_3, 0.545%), zinc (ZnO, 0.141%), manganese (MnO, 0.0573%), copper (CuO, 0.0464%), titanium (TiO_2, 0.0593%), chromium (Cr_2O_3, 0.0258%), rubidium (Rb_2O, 0.0519%), strontium (SrO, 0.371%), tin (SnO_2, 0.0924%), and bromine (Br, 0.228%). Many of these elements serve as essential micronutrients, functioning as cofactors for antioxidant and redox-related enzymes such as superoxide dismutase and various oxidoreductases. In particular, iron, zinc, manganese, and copper play critical roles in electron transport, oxidative metabolism, and cellular defense against oxidative stress. The detection of bromine and rubidium, which are less frequently reported in

medicinal plants, adds further depth and novelty to the elemental characterization of *A. aspera*.

Tantalum oxide (Ta_2O_5) was not detected under the present experimental conditions. Overall, the XRF analysis demonstrates that *Achyranthesaspera* possesses a diverse and well-balanced elemental composition encompassing essential macro-, micro-, and trace elements. This comprehensive mineral profile may act synergistically with phytochemical constituents to contribute to the plant's reported pharmacological activities and traditional medicinal applications. Moreover, the elemental data generated in this study provide a useful reference for quality control, safety assessment, and pharmacognostic standardization of *A. aspera*–based phytopharmaceutical formulations.

Table 2: Elemental composition of *Achyranthesaspera* Linn.powder determined by X-ray fluorescence (XRF) spectroscopy

Oxide	Mass %	Probable Elemental Form	Remarks / Biological Significance
MgO	5.93	Magnesium	Cofactor in enzymatic reactions, essential for chlorophyll structure
Al_2O_3	1.95	Aluminium	Trace element, may aid in cell wall stability
SiO_2	2.35	Silicon	Structural integrity, resistance to pathogens
P_2O_5	2.00	Phosphorus	Vital for energy metabolism (ATP)
SO_3	2.70	Sulphur	Present in amino acids and coenzymes
Cl	15.00	Chlorine	Maintains ionic balance and osmotic potential
K_2O	44.90	Potassium	Major plant macronutrient; enzyme activation, water balance
CaO	23.60	Calcium	Structural role in cell wall, signal transduction
TiO_2	0.0593	Titanium	Trace metal, may influence metabolic activity
Cr_2O_3	0.0258	Chromium	Trace element; excessive amounts may be toxic
MnO	0.0573	Manganese	Cofactor for antioxidant enzymes (superoxide dismutase)
Fe_2O_3	0.545	Iron	Crucial for chlorophyll synthesis and redox reactions
CuO	0.0464	Copper	Involved in electron transport and oxidative enzymes
ZnO	0.141	Zinc	Structural and catalytic cofactor for numerous enzymes
Br	0.228	Bromine	Trace halogen element, rarely reported in plants
Rb_2O	0.0519	Rubidium	Trace element; chemical analog of potassium
SrO	0.371	Strontium	Minor element, sometimes substitutes calcium
SnO_2	0.0924	Tin	Trace metal, no major biological role known
Ta_2O_5	ND	Tantalum	Not detected

3.4. UV-Visible spectral analysis

The ultraviolet–visible (UV–Vis) absorption spectrum of the hexane extract of *Achyranthesaspera* Linn. was recorded over the wavelength range of 190–800 nm using a Shimadzu UV-3600 double-beam spectrophotometer (Figure 3). The spectrum exhibited multiple well-defined absorption features, reflecting the presence of diverse chromophoric and auxochromic groups associated with different classes of phytoconstituents. A prominent absorption maximum (λ_{max}) was observed at approximately 274 nm, accompanied by shoulder bands in the 230–260 nm region and a broad absorption feature centered around 340 nm, indicating the coexistence of conjugated π–π* and n–π* electronic transitions.

The intense absorption observed in the 200–300 nm region is characteristic of π–π* transitions arising from aromatic C=C bonds and conjugated systems, which are commonly associated with flavonoids, phenolic acids, and terpenoid compounds. The shoulder near 340 nm suggests the presence of extended conjugation, a spectral feature typically attributed to polyphenolic structures and flavone-type compounds. The relatively high absorbance intensity, reaching approximately 2.85 absorbance units at shorter wavelengths, further supports the abundance of unsaturated and aromatic constituents within the plant extract.

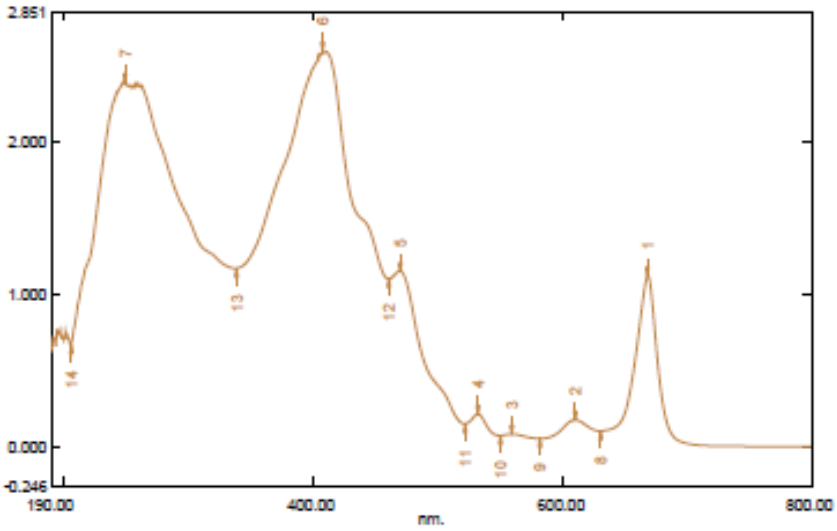

Figure 3: Ultraviolet–visible (UV–Vis) absorption spectrum of the hexane extract of *Achyranthesaspera* Linn. recorded over the wavelength range of 190–800 nm, showing characteristic absorption bands associated with conjugated aromatic and polyphenolicphytoconstituents.

Notably, the absence of sharp or intense absorption bands beyond 400 nm indicates negligible interference from chlorophylls or other colored pigments in the analyzed fraction, confirming that the hexane extract predominantly contains non-pigmented secondary metabolites. The overall spectral profile is consistent with previously reported UV–Vis characteristics of *A. aspera* extracts, which commonly exhibit absorption maxima in the range of 270–350 nm corresponding to phenolic and flavonoid chromophores, thereby reinforcing the validity of the present findings.

3.5. LCMS Detection and Evaluation

The alkaloid-rich fraction of *Achyranthesaspera* Linn.was characterized by liquid chromatography–mass spectrometry (LC–MS) using a Waters XEVO TQD triple-quadrupole instrument operated under both positive (ES^+) and negative (ES^-) electrospray ionization modes. The total ion chromatograms (TICs) (Figure 4) exhibited multiple well-resolved signals across a retention time window of approximately 2.3–11.9 min, indicating a chemically diverse mixture of alkaloidal constituents with varying polarity and ionization behavior.

Several prominent chromatographic peaks were consistently detected at retention times around 2.35, 3.76, 4.62, 6.28, 7.48, 8.16, 9.23, 10.58, and 11.87 min, each corresponding to distinct molecular ion species observed in the associated mass spectra. The positive ionization mode produced the highest overall response, with maximum signal intensities reaching ~2.94×10^8 a.u., reflecting the abundance of protonated alkaloids in the extract. In contrast, the negative ion mode yielded moderate but clearly discernible responses (approximately 1.6×10^7 a.u.), confirming that a subset of the detected compounds possesses acidic or amphoteric functional groups capable of deprotonation.

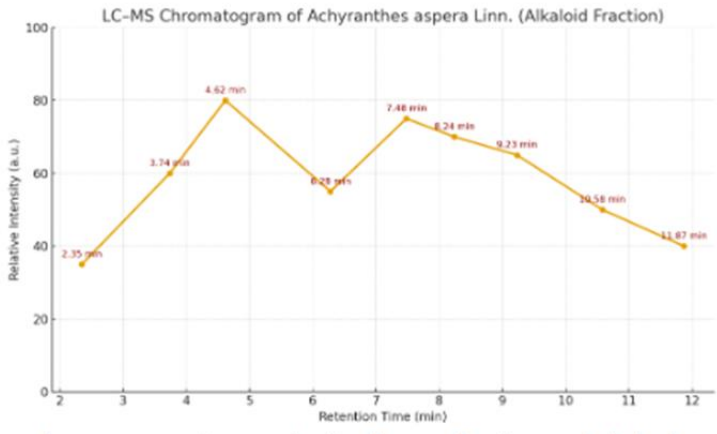

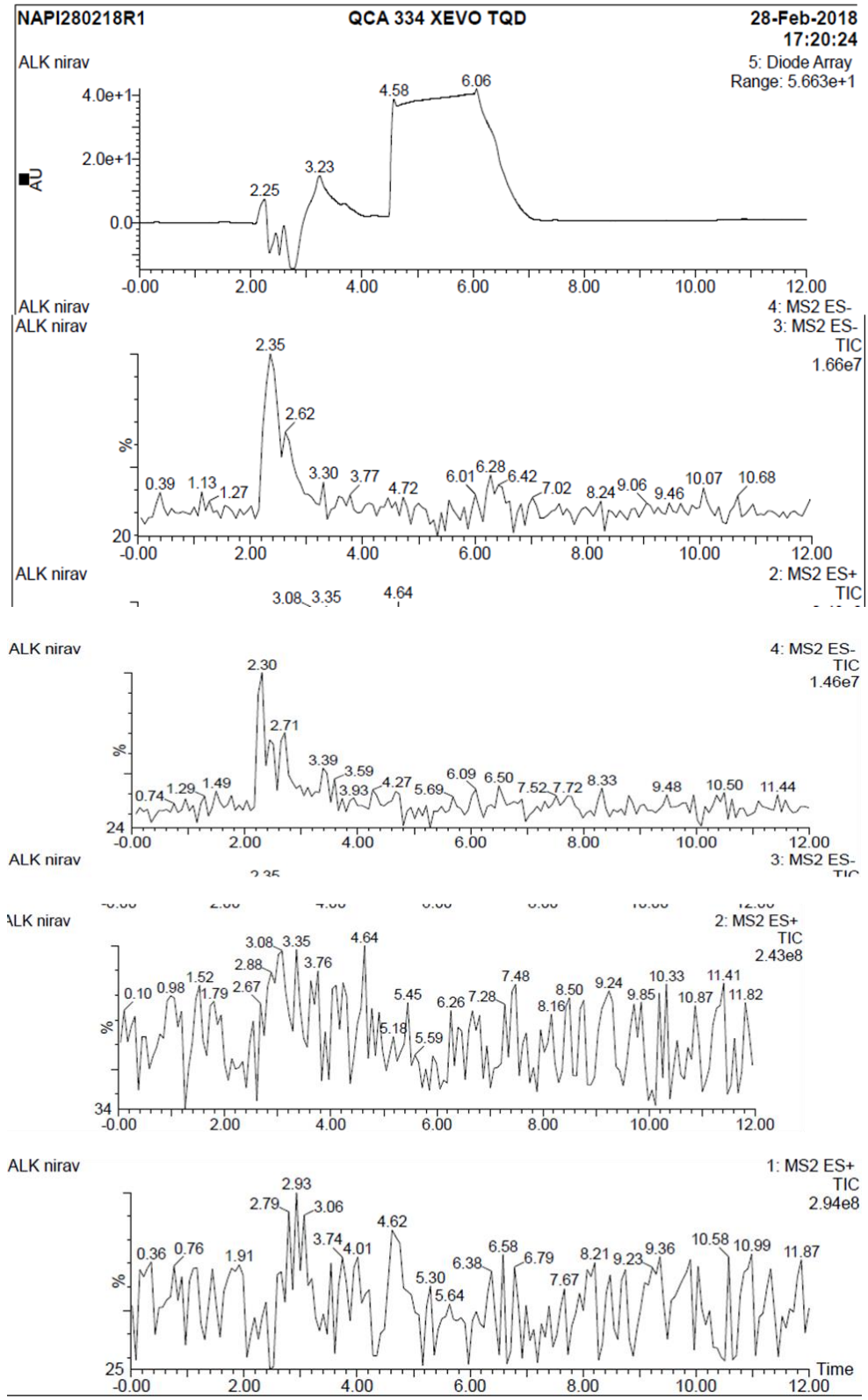

Figure 4: LC–MS total ion chromatograms (TIC) of the alkaloid fraction of *Achyranthesaspera* Linn. recorded in positive (ES^+) and negative (ES^-) electrospray ionization modes, showing multiple well-resolved peaks between 2.3 and 11.8 min, indicative of chemically diverse alkaloid constituents.

Interpretation of the mass spectral fragmentation patterns (Table 4) revealed the presence of multiple classes of alkaloidal compounds. Early-eluting peaks in the 2.35–2.62 min range detected in ES^- mode, characterized by low *m/z* fragments (59.2, 161.1, 217.2, and 331.2), are suggestive of simple aliphatic amines or amide-type derivatives. Peaks eluting between 3.74 and 4.62 min in ES^+ mode showed diagnostic ions at *m/z* 99.1, 201.3, 334.4, and 361.4, consistent with indole-type or pyridine alkaloids. The mid-retention region (5.18–6.28 min) was dominated by ions at *m/z* 219.3, 345.4, and 510.0, indicating the possible presence of steroidal or triterpenoid alkaloids.

At longer retention times, peaks observed between 7.48 and 8.24 min displayed high-mass ions (*m/z* 573.9, 699.5, and 745.5), which may be attributed to glycosidic or polymeric alkaloid structures. Further late-eluting components in the 9.23–10.68 min range exhibited very high *m/z* values (941.7, 1039.2, and 1095.3), suggesting dimeric alkaloids or alkaloid–flavonoid conjugates. The final peaks detected between 11.44 and 11.87 min, with molecular ions extending up to *m/z* 1195.6, are indicative of highly conjugated glycosidic or triterpenoid alkaloid assemblies.

Overall, the LC–MS results demonstrate that *Achyranthesaspera* contains a broad spectrum of alkaloidal constituents ranging from low-molecular-weight amines to complex high-mass conjugates. This chemical diversity provides strong molecular evidence supporting the plant's reported pharmacological activities and highlights its potential as a rich source of structurally varied bioactive alkaloids.

Table 4: LC–MS Identification of Compounds

Retention time (min)	Mode	Major m/z fragments	Proposed compound class / interpretation
2.35 – 2.62	ES^-	59.2, 161.1, 217.2, 331.2	Simple aliphatic amines, amide derivatives
3.74 – 4.62	ES^+	99.1, 201.3, 334.4, 361.4	Indole-type or pyridine alkaloids
5.18 – 6.28	ES^+	219.3, 345.4, 510.0	Steroidal or triterpenoid alkaloids
7.48 – 8.24	ES^+	573.9, 699.5, 745.5	Glycosidic or polymeric alkaloids
9.23 – 10.68	ES^+	941.7, 1039.2, 1095.3	Dimeric alkaloids / alkaloid-flavonoid conjugates
11.44 – 11.87	ES^+	1122.5, 1195.6	High-mass glycosidic or triterpenoid conjugates

3.6. Mass Spectral Interpretation

The mass spectra corresponding to the dominant chromatographic peaks (Figure 4) revealed a broad distribution of *m/z* values ranging from 59 to 1195 amu, reflecting the presence of structurally diverse alkaloidal constituents in *Achyranthesaspera*. Several intense and recurrent fragment ions were observed at *m/z* 59.2, 99.1, 161.1, 201.3, 219.3, 334.4, 361.4, 510.0, 699.5, 745.5, 1039.2, 1095.3, 1122.5, and 1195.6 in both positive and negative electrospray ionization modes, confirming consistent fragmentation behavior across different ionization conditions.

Low-molecular-weight fragments in the *m/z* range of 59–219 are characteristic of simple alkyl, amine, and amide moieties, providing clear evidence for the abundance of nitrogen-containing secondary metabolites typical of *Achyranthes* species. Fragment ions in the intermediate mass region (*m/z* 334–510) are likely associated with partially substituted indole, pyridine, or steroidal alkaloid frameworks, which commonly undergo fragmentation via C–N and C–O bond cleavage pathways. The detection of high-mass ions exceeding *m/z* 700, extending up to *m/z* 1195, suggests the presence of more complex molecular architectures, such as dimeric alkaloids or glycosidic conjugates, including triterpenoid–alkaloid glycosides. Such high-molecular-weight alkaloids have been previously reported in *A. aspera* and are considered significant contributors to its bioactivity.

Further analysis of the MS^2 spectra acquired in both ionization polarities consistently showed repetitive daughter ions at *m/z* 59.2, 99.1, 161.1, and 201.3. These fragments can therefore be regarded as diagnostic ions for the alkaloid-rich fraction of *A. aspera*, providing a reliable mass spectrometric fingerprint for its chemical characterization and future quality control studies.

4. Discussion

The FTIR spectral profile offers a comprehensive chemical "fingerprint" that effectively complements the chromatographic, spectrometric, and elemental analyses. The strong representation of hydroxyl (–OH), carbonyl (C=O), and aromatic functional groups indicates that the extract is particularly enriched with polar phytochemicals, including phenolics, flavonoids, glycosides, and related oxygenated metabolites. These classes of compounds are widely associated with antioxidant, anti-inflammatory, and cytoprotective activities. In parallel, the presence of aliphatic C–H stretching vibrations (CH_2 and CH_3) reflects the coexistence of non-polar constituents such as terpenoids, sterols, and fatty acid derivatives, which are known to contribute to membrane stabilization and modulation of inflammatory pathways. This dual chemical character highlights the broad phytochemical diversity of *Achyranthesaspera*.

Elemental profiling by XRF revealed a marked predominance of potassium oxide (K_2O, 44.9%) and calcium oxide (CaO, 23.6%), demonstrating that *A. aspera* is exceptionally rich in essential macronutrients required for plant physiology and potentially beneficial for human nutrition. Substantial levels of chlorine (15.0%), magnesium (5.93%), and sulphur (2.70%) further support the plant's biochemical activity, as these elements are integral to enzyme activation, osmoregulation, and sulfur-containing biomolecules. The detection of trace elements such as iron, manganese, zinc, and copper—although present in minor concentrations—is particularly relevant, as these metals play critical roles in redox homeostasis, enzymatic catalysis, and mitigation of oxidative stress. Their presence is consistent with the well-documented antioxidant and anti-inflammatory properties of *A. aspera*. Minor oxides, including TiO_2, Cr_2O_3, and SnO_2, were observed only in trace amounts and are most likely derived from natural soil uptake rather than intrinsic toxicity.

The overall XRF elemental pattern closely aligns with earlier reports by Mandal et al. (2025), who documented elevated levels of potassium, calcium, and magnesium in *A. aspera*, indicating a reproducible and characteristic mineral signature. Importantly, the absence of hazardous heavy metals at toxic levels supports the safety of this plant for phytopharmaceutical and nutraceutical applications, while simultaneously underscoring its nutritional and therapeutic potential.

The UV–Visible spectroscopic profile provides an additional, rapid fingerprint for the phytochemical identity of *A. aspera*. Strong absorption bands in the ultraviolet region are attributable to π–π* electronic transitions within conjugated aromatic systems, which are characteristic of flavonoids, phenolic compounds, saponins, and triterpenoids. These observations are in excellent agreement with the FTIR and chromatographic data and directly support the antioxidant potential of the extract, as extended conjugation enhances radical-scavenging and electron-donating capabilities. Collectively, the UV–Vis data reinforce the chemical complexity of *A. aspera* and validate its long-standing ethnomedicinal use by confirming the presence of multiple bioactive chromophores.

The LC–MS analysis further substantiates the complexity of the alkaloid profile of *Achyranthesaspera Linn.* The simultaneous detection of low- and high-molecular-weight ions reflects a heterogeneous mixture of simple amine-based alkaloids alongside structurally elaborate triterpenoid- and glycosidic-linked nitrogenous compounds. Prominent ions in the *m/z* range of 200–600 are consistent with alkaloids commonly reported in the genus, including achyranthine-related structures, ecdysterone derivatives, and betaine-like nitrogenous bases. These constituents are known to contribute to the plant's adaptogenic and anti-inflammatory properties. Notably, the presence of high-mass fragment ions above *m/z* 1000 points toward polymeric, dimeric, or sugar-conjugated alkaloids, corroborating earlier phytochemical and HPLC findings that suggested the occurrence of saponin–alkaloid complexes. This high-mass region (*m/z* 1039–1195) is of particular pharmacological significance, as glycosylated and conjugated alkaloids often exhibit improved bioavailability, enhanced biological potency, and multifunctional therapeutic effects, including hepatoprotective and immunomodulatory activities.

When interpreted collectively, the FTIR, UV–Vis, XRF, and LC–MS datasets provide a coherent and multidimensional chemical picture of *A. aspera*. The integrated evidence confirms the coexistence of nitrogenous alkaloids, oxygen-rich polyphenols, conjugated aromatic systems, and essential mineral elements, thereby offering molecular-level validation of the plant's ethnopharmacological relevance and supporting its continued exploration for phytotherapeutic development.

5. Conclusion

The FTIR spectral profile offers a comprehensive chemical "fingerprint" that effectively complements the chromatographic, spectrometric, and elemental analyses. The strong representation of hydroxyl (–OH), carbonyl (C=O), and aromatic functional groups indicates that the extract is particularly enriched with polar phytochemicals, including phenolics, flavonoids, glycosides, and related oxygenated metabolites. These classes of compounds are widely associated with antioxidant, anti-inflammatory, and cytoprotective activities. In parallel, the presence of aliphatic C–H stretching vibrations (CH_2 and CH_3) reflects the coexistence of non-polar constituents such as terpenoids, sterols, and fatty acid derivatives, which are known to contribute to membrane stabilization and modulation of inflammatory pathways. This dual chemical character highlights the broad phytochemical diversity of *Achyranthesaspera*.

Elemental profiling by XRF revealed a marked predominance of potassium oxide (K_2O, 44.9%) and calcium oxide (CaO, 23.6%), demonstrating that *A. aspera* is exceptionally rich in essential macronutrients required for plant physiology and potentially beneficial for human nutrition. Substantial levels of chlorine (15.0%), magnesium (5.93%), and sulphur (2.70%) further support the plant's biochemical activity, as these elements are integral to enzyme activation, osmoregulation, and sulfur-containing biomolecules. The detection of trace elements such as iron, manganese, zinc, and copper—although present in minor concentrations—is particularly relevant, as these metals play critical roles in redox homeostasis, enzymatic catalysis, and mitigation of oxidative stress. Their presence is consistent with the well-documented antioxidant and anti-inflammatory properties of *A. aspera*. Minor oxides, including TiO_2, Cr_2O_3, and SnO_2, were observed only in trace amounts and are most likely derived from natural soil uptake rather than intrinsic toxicity.

The overall XRF elemental pattern closely aligns with earlier reports by Mandal et al. (2025), who documented elevated levels of potassium, calcium, and magnesium in *A. aspera*, indicating a reproducible and characteristic mineral signature. Importantly, the absence of hazardous heavy metals at toxic levels supports the safety of this plant for phytopharmaceutical and nutraceutical applications, while simultaneously underscoring its nutritional and therapeutic potential.

The UV–Visible spectroscopic profile provides an additional, rapid fingerprint for the phytochemical identity of *A. aspera*. Strong absorption bands in the ultraviolet region are attributable to π–π* electronic transitions within conjugated aromatic systems, which are characteristic of flavonoids, phenolic compounds, saponins, and triterpenoids. These observations are in excellent agreement with the FTIR and chromatographic data and directly support the antioxidant potential of the extract, as extended conjugation enhances radical-scavenging and electron-donating capabilities. Collectively, the UV–Vis data reinforce the chemical complexity of *A. aspera* and validate its long-standing ethnomedicinal use by confirming the presence of multiple bioactive chromophores.

The LC–MS analysis further substantiates the complexity of the alkaloid profile of *Achyranthesaspera Linn.* The simultaneous detection of low- and high-molecular-weight ions reflects a heterogeneous mixture of simple amine-based alkaloids alongside structurally elaborate triterpenoid- and glycosidic-linked nitrogenous compounds. Prominent ions in the *m/z* range of 200–600 are consistent with alkaloids commonly reported in the genus, including achyranthine-related structures, ecdysterone derivatives, and betaine-like nitrogenous bases. These constituents are known to contribute to the plant's adaptogenic and anti-inflammatory properties.

Notably, the presence of high-mass fragment ions above *m/z* 1000 points toward polymeric, dimeric, or sugar-conjugated alkaloids, corroborating earlier phytochemical and HPLC findings that suggested the occurrence of saponin–alkaloid complexes. This high-mass region (*m/z* 1039–1195) is of particular pharmacological significance, as glycosylated and conjugated alkaloids often exhibit improved bioavailability, enhanced biological potency, and multifunctional therapeutic effects, including hepatoprotective and immunomodulatory activities.

When interpreted collectively, the FTIR, UV–Vis, XRF, and LC–MS datasets provide a coherent and multidimensional chemical picture of *A. aspera*. The integrated evidence confirms the coexistence of nitrogenous alkaloids, oxygen-rich polyphenols, conjugated aromatic systems, and essential mineral elements, thereby offering molecular-level validation of the plant's ethnopharmacological relevance and supporting its continued exploration for phytotherapeutic development.

Ethics approval and consent to participate

This study was conducted in Accordance with Applicable ethical Guideline and regulation. As the preset research did not involve human participant or anima,formal ethical approval and informed consent were not required.

Funding

This research did not receive any specific grant from funding agencies in the public, commercial, or not-for-profit sectors.

Availability of data and materials

The Datasets analyzed in the current study were generated during the author's dissertation work in 2018. The data are available from the corresponding author upon reasonable request.

Declaration of competing interest

The authors declare they have no known competing financial interests or personal relationships that could have influenced the work reported in this paper.

References

[1]. Dettmer, K., Aronov, P.A., Hammock, B.D., 2007. Mass spectrometry-based metabolomics. Mass Spectrom. Rev. 26, 51–78. https://doi.org/10.1002/mas.20108

[2]. Dutt, V., Thakur, S., Dhar, V., Sharma, A., 2010. The genus Gelsemium: An update. Pharmacogn. Rev. 4, 185. https://doi.org/10.4103/0973-7847.70916

[3]. Gokhale, A.B., Damre, A.S., Kulkarni, K.R., Saraf, M.N., 2002. Preliminary evaluation of anti-inflammatory and anti-arthritic activity of S. lappa, A. speciosa and A. aspera. Phytomedicine 9, 433–437. https://doi.org/10.1078/09447110260571689

[4]. Harborne, J.B., Harborne, J.B., 1998. Phytochemical methods: a guide to modern techniques of plant analysis, 3rd ed. ed. Chapman and Hall, London Weinheim.

[5]. Isha Talhar, I.T., Vaibhav Panchabhudhe, V.P., Bhavana P. Raut, B.P.R., 2025. A Review on Potential of Achyranthes Aspera Linn. Int. J. Pharm. Res. Appl. 10, 893–902. https://doi.org/10.35629/4494-1003893902

[6]. Lindon, J.C., Tranter, G.E., Koppenaal, D.W. (Eds.), 2017. Encyclopedia of spectroscopy and spectrometry, Third edition. ed. Elsevier, Academic Press, Amsterdam Boston Heidelberg.

[7]. Nargatti, P., Patil, S., Wadkar, K., 2021. Phytochemical Profile and Pharmacological Aspects of Achyranthes aspera Linn- An Overview. J. Pharm. Res. Int. 187–206. https://doi.org/10.9734/jpri/2021/v33i34B31860

[8]. Niessen, W.M.A., 2006. Liquid Chromatography-Mass Spectrometry, 0 ed. CRC Press. https://doi.org/10.1201/9781420014549

[9]. Qureshi, S., Solanki, H., 2022. FT-IR ANALYSIS OF THE CRUDE SAMPLE OF ACHYRANTHES ASPERA L. LEAVES. Int. Assoc. Biol. Comput. Dig. 1, 166–167. https://doi.org/10.56588/iabcd.v1i2.64

[10]. Sapkota, Y., McDonald, L.M., Griggs, T.C., Basden, T.J., Drake, B.L., 2019. Portable X-Ray Fluorescence Spectroscopy for Rapid and Cost-Effective Determination of Elemental Composition of Ground Forage. Front. Plant Sci. 10, 317. https://doi.org/10.3389/fpls.2019.00317

[11]. Silverstein, R.M., Webster, F.X., Kiemle, D.J., Bryce, D.L., 2015. Spectrometric identification of organic compounds, Eighth edition. ed. Wiley, Hoboken, NJ.

[12]. Singh, R.K., Verma, P.K., Kumar, A., Kumar, S., Acharya, A., 2021. Achyranthes aspera L. leaf extract induced anticancer effects on Dalton's Lymphoma via regulation of PKCα signaling pathway and mitochondrial apoptosis. J. Ethnopharmacol. 274, 114060. https://doi.org/10.1016/j.jep.2021.114060

[13]. Skoog, D.A., Holler, F.J., Crouch, S.R., 2018. Principles of instrumental analysis, 7. edition. ed. Cengage Learning, Boston, MA.

[14]. Snyder, L.R., Kirkland, J.J., Dolan, J.W., 2009. Introduction to Modern Liquid Chromatography, 1st ed. Wiley. https://doi.org/10.1002/9780470508183

[15]. Sofowora, A., Ogunbodede, E., Onayade, A., 2013. The role and place of medicinal plants in the strategies for disease prevention. Afr. J. Tradit. Complement. Altern. Med. 10, 210–229. https://doi.org/10.4314/ajtcam.v10i5.2

[16]. Stahl, E. (Ed.), 1969. Thin-Layer Chromatography. Springer Berlin Heidelberg, Berlin, Heidelberg. https://doi.org/10.1007/978-3-642-88488-7

[17]. Stalikas, C.D., 2007. Extraction, separation, and detection methods for phenolic acids and flavonoids. J. Sep. Sci. 30, 3268–3295. https://doi.org/10.1002/jssc.200700261

[18]. Towett, E.K., Shepherd, K.D., Lee Drake, B., 2016. Plant elemental composition and portable X-ray fluorescence (pXRF) spectroscopy: quantification under different analytical parameters. X-Ray Spectrom. 45, 117–124. https://doi.org/10.1002/xrs.2678

[19]. Vijaya Kumar, S., Sankar, P., Varatharajan, R., 2009. Anti-inflammatory activity of roots of *Achyranthes aspera*. Pharm. Biol. 47, 973–975. https://doi.org/10.1080/13880200902967979

[20]. Wolfender, J.-L., Marti, G., Thomas, A., Bertrand, S., 2015. Current approaches and challenges for the metabolite profiling of complex natural extracts. J. Chromatogr. A 1382, 136–164. https://doi.org/10.1016/j.chroma.2014.10.091